JOURNAL OF NATURAL PRODUCTS

Article

pubs.acs.org/jnp

Spiroindole Alkaloids and Spiroditerpenoids from *Aspergillus duricaulis* and Their Potential Neuroprotective Effects

Jaeyoung Kwon,[†] Young Hye Seo,[†] Jae-Eun Lee,[‡] Eun-Kyoung Seo,[§] Shen Li,[⊥] Yuanqiang Guo,[⊥] Seung-Beom Hong,[∥] So-Young Park,*[,‡] and Dongho Lee*[,†]

[†]Department of Biosystems and Biotechnology, College of Life Sciences and Biotechnology, Korea University, Seoul 02841, Republic of Korea

[‡]Laboratory of Pharmacognosy, College of Pharmacy, Dankook University, Cheonan 31116, Republic of Korea

[§]College of Pharmacy, Ewha Womans University, Seoul 03760, Republic of Korea

[⊥]Tianjin Key Laboratory of Molecular Drug Research, College of Pharmacy, Nankai University, Tianjin 300071, People's Republic of China

[∥]Korean Agricultural Culture Collection, National Academy of Agricultural Science, Wanju 55365, Republic of Korea

Supporting Information

ABSTRACT: Six new spiroindole alkaloids (**1**−**6**) and two new spiroditerpenoids (**7** and **8**) were isolated from an EtOAc extract of *Aspergillus duricaulis* culture media together with five known compounds. The structures of the isolated compounds were elucidated by analysis of NMR and MS data, and the absolute configurations of compounds **1**−**8** were confirmed by CD spectroscopic methods. All isolated compounds were evaluated for their inhibition of beta-amyloid (Aβ) aggregate-induced toxicity in PC12 cells and Aβ aggregation. Compounds **8**−**11** efficiently protected PC12 cells against Aβ aggregate-induced toxicity, but only compound **9** inhibited Aβ aggregation. On the other hand, compounds **4** and **5** exhibited moderate inhibitory effects on Aβ aggregation, but did not protect the cells from Aβ aggregate-induced toxicity. Preincubating Aβ monomers with compounds **4** and **5** rescued PC12 cells against Aβ aggregate-induced toxicity by reducing neurotoxic Aβ aggregates. Compound **9** inhibited both Aβ aggregate-induced toxicity and Aβ aggregation.

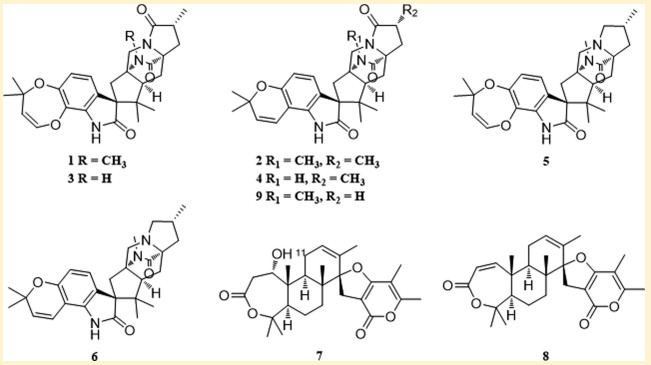

Alzheimer's disease (AD) is characterized by progressive loss of memory and other cognitive functions and is one of the most serious neurodegenerative disorders in the elderly population.[1] The pathologic hallmark of AD is the extracellular deposition of the beta-amyloid (Aβ) peptide forming senile plaques. Aβ originates from the sequential proteolytic cleavage of the amyloid precursor protein by β- and γ-secretases.[2] The overproduction of Aβ leads to the accumulation and aggregation of Aβ, which trigger neuronal death through oxidative stress, energy depletion, inflammation, and apoptosis.[3] Several potential therapeutic strategies have been suggested, and some medicines, such as memantine, tacrine, donepezil, rivastigmine, and galantamine, have been developed.[4] Although these medicines are expected to slow down the progression of AD, the number of people with this disease is increasing and is expected to increase to 114 million by 2050 because these drugs improve only some of the disease symptoms and a radical treatment has yet to be found.[4,5] Natural products with anti-AD properties have attracted much attention during the recent decade.[4] Among them, fungal-derived secondary metabolites from terrestrial and marine fungi may be an important therapeutic approach for AD because of their structural diversity and biological activity.[6]

In our continuous search for natural-product-derived neuroprotective compounds,[7−9] an EtOAc-soluble extract of *Aspergillus duricaulis* culture media protected PC12 cells against Aβ aggregate-induced toxicity. Six new spiroindole alkaloids (**1**−**6**) and two new spiroditerpenoids (**7** and **8**), along with five known compounds, 16-oxo-paraherquamide B (**9**),[10] setosusin (**10**),[11] 2,2-dimethyl-2*H*-1-chromene-6-carboxylate (**11**),[12] deacetyl-dehydrated setosusin,[11] and 4-hydroxy-3-prenylbenzoic acid,[13] were subsequently isolated from the extract. Compounds **4**, **5**, and **9** inhibited Aβ aggregation with moderate activity, whereas compounds **8**−**11** protected PC12 cells against Aβ aggregate-induced toxicity. The inhibition of Aβ aggregation after pretreatment of Aβ monomers with compounds **4** and **5** rescued the cells against Aβ, even though these compounds did not inhibit toxicity induced by already

Received: June 8, 2015

DOI: 10.1021/acs.jnatprod.5b00508
J. Nat. Prod. XXXX, XXX, XXX−XXX

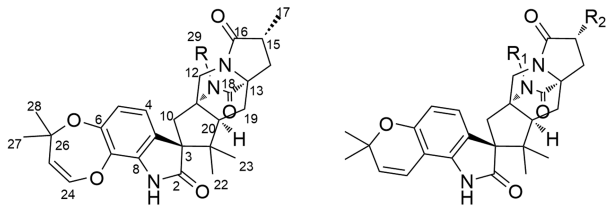

1 R = CH_3
3 R = H

2 R_1 = CH_3, R_2 = CH_3
4 R_1 = H, R_2 = CH_3
9 R_1 = CH_3, R_2 = H

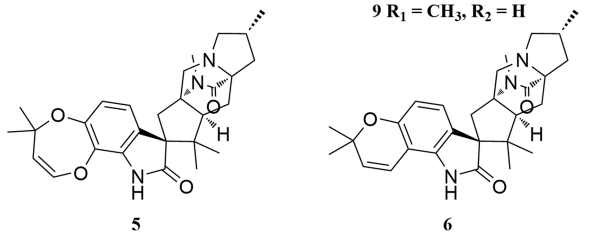

5 6

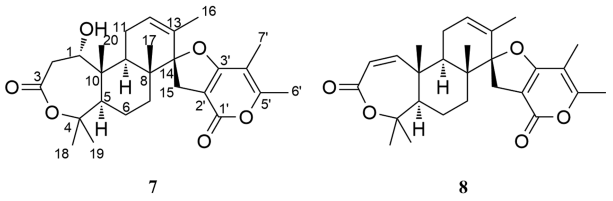

7 8

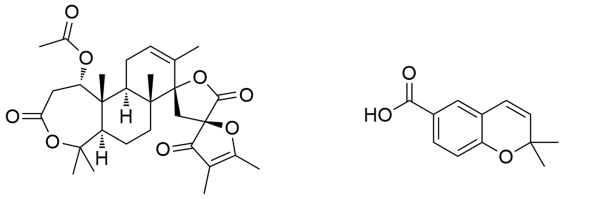

10 11

formed Aβ aggregates. Compound **9**, however, exhibited both activities.

RESULTS AND DISCUSSION

Compound **1** was isolated as a white, amorphous solid. Its molecular formula of $C_{28}H_{33}N_3O_5$ was deduced from HRESIMS analysis, suggesting 14 degrees of unsaturation. The ^{1}H NMR data (Table 1) displayed six methyl groups including an amide *N*-methyl [δ_H 3.10 (3H, s, NMe-29), 1.46 (3H, s, Me-27), 1.44 (3H, s, Me-28), 1.25 (3H, d, *J* = 7.0 Hz, Me-17), 1.08 (3H, s, Me-22), and 0.87 (3H, s, Me-23)], four methylene groups [δ_H 3.82 (1H, d, *J* = 12.0 Hz, H-12a), 3.50 (1H, d, *J* = 12.5 Hz, H-12b), 2.81 (1H, d, *J* = 15.5 Hz, H-10a), 2.61 (1H, dd, *J* = 13.5, 6.0 Hz, H-14a), 2.08 (1H, dd, *J* = 13.5, 10.0 Hz, H-14b), 2.02 (1H, d, *J* = 15.5 Hz, H-10b), 1.94 (1H, dd, *J* = 12.5, 11.0 Hz, H-19a), and 1.79 (1H, dd, *J* = 12.5, 10.5 Hz, H-19b)], and six methine groups, of which two were aromatic and two olefinic [δ_H 6.81 (1H, d, *J* = 8.0 Hz, H-4), 6.71 (1H, d, *J* = 8.0 Hz, H-5), 6.31 (1H, d, *J* = 7.5 Hz, H-24), 4.90 (1H, d, *J* = 7.5 Hz, H-25), 3.33 (1H, t, *J* = 10.5 Hz, H-20), and 2.73 (1H, m, H-15)]. The ^{13}C NMR data (Table 1) showed 28 carbon signals, including six methyl, six methine, four methylene, three amide carbonyl, three oxygenated tertiary, three N-containing tertiary, and three quaternary carbons. The 1D NMR data of **1** were comparable to those of paraherquamide H,[14] which contains heptacyclic carbon frameworks consisting a bicyclo[2,2,2]diazaoctane core joined to a substituted proline moiety and a dioxygenated seven-membered ring with a 1,2-disubstituted olefin joined to a spiroindole moiety. The only difference found was the change of the position of the methyl group in **1** from C-14 to C-15. The HMBC cross-peaks of Me-17/C-14, C-15, and C-16 indicated that the methyl group of the terminal proline unit in **1** was located at C-15. The gross structure of **1** was further confirmed by additional 2D NMR data (Figure 1). Accordingly, the structure of the new compound **1** was elucidated as shown and has been given the trivial name paraherquamide J.

The molecular formula of compound **2** was determined as $C_{28}H_{33}N_3O_4$ from HRESIMS analysis. Its ^{1}H and ^{13}C NMR data (Table 1) were similar to those of **1**, which has a typical paraherquamide skeleton, except that the dioxygenated seven-membered ring in **1** was changed to a monooxygenated six-membered ring [δ_H 6.29 (1H, d, *J* = 10.0 Hz, H-24) and 5.72 (1H, d, *J* = 10.0 Hz, H-25)]. The structure of the new compound **2** was confirmed by the 2D NMR data and elucidated as paraherquamide K.

The ^{1}H and ^{13}C NMR spectroscopic data of compounds **3** (Table 1) and **4** (Table 2) were superimposable to those of **1** and **2**, respectively, except for the disappearance of the amide *N*-methyl groups, which was confirmed by the presence of the amide proton signals of **3** [δ_H 6.97 (1H, s, NH-29)] and **4** [δ_H 6.95 (1H, s, NH-29)] and the HMBC cross-peaks from NH-29 to C-13. Finally, the entire structures were confirmed by HRESIMS analyses. Consequently, the new compounds **3** and **4** were determined to be 29-*N*-demethylparaherquamide J and 29-*N*-demethylparaherquamide K, respectively.

Compounds **5** and **6** had the molecular formulas $C_{28}H_{35}N_3O_4$ and $C_{28}H_{35}N_3O_3$, respectively. According to their ^{1}H and ^{13}C NMR data (Table 2), both compounds have the same paraherquamide skeleton as that of **1** and **2** except for the absence of the carbonyl groups at C-16 in **5** and **6**. The presence of the methylene proton signals in **5** [δ_H 3.06 (1H, m, H-16a) and 1.79 (1H, m, H-16b)] and **6** [δ_H 3.06 (1H, m, H-16a) and 1.79 (1H, m, H-16b)], the ^{1}H−^{1}H COSY cross-peaks of H-15/H-16, and the HMBC cross-peaks of H-16/C-13 and C-14 and Me-17/C-14, C-15, and C-16 confirmed the structure of the terminal proline unit. Thus, the new compounds **5** and **6** were determined as 16-deoxo-paraherquamide J and 16-deoxo-paraherquamide K, respectively.

The relative configurations of all stereogenic centers in compounds **1**−**6** were the same as those of the previously reported paraherquamides as concluded from the close resemblance of the ^{1}H and ^{13}C chemical shifts and NOESY data.[15,16] The NOESY correlations of H-4/H-10b and Me-22 indicated the relative configuration of the spiro center at C-3, and those of H-12a/Me-22 and of H-20/Me-23 indicated that H-12 and H-20 were *trans*-diaxial (Figure 2). Furthermore, the additional NOESY correlations allowed stereospecific proton assignments of all germinal proton pairs. CD spectroscopy is considered decisive for the absolute configuration of spiroindole alkaloids.[17,18] The CD spectra of **1**−**6** showed negative Cotton effects at 260−280 nm (Supporting Information, S25), which indicated that each compound has the same 3*R* configuration. Consequently, the absolute configurations of compounds **1**−**4** were 3*R*, 11*S*, 13*R*, 15*R*, and 20*S*, and those of compounds **5** and **6** were 3*R*, 11*S*, 13*S*, 15*R*, and 20*S*.

Compound **7**, isolated as a white, amorphous solid, had a molecular formula of $C_{27}H_{36}O_6$ as determined by HRESIMS analysis, suggesting 10 degrees of unsaturation. The ^{1}H NMR spectroscopic data (Table 3) revealed seven methyl groups [δ_H 2.22 (3H, s, Me-7′), 1.93 (3H, s, Me-6′), 1.66 (3H, s, Me-16),

DOI: 10.1021/acs.jnatprod.5b00508
J. Nat. Prod. XXXX, XXX, XXX−XXX

Table 1. NMR Spectroscopic Data of Compounds 1−3

	1[a]			2[a]			3[a]		
position	δ_C, type	δ_H, mult (J in Hz)	HMBC[b]	δ_C, type	δ_H, mult (J in Hz)	HMBC[b]	δ_C, type	δ_H, mult (J in Hz)	HMBC[b]
2	182.1, C			183.7, C			182.3, C		
3	63.3, C			62.5, C			63.1, C		
4	120.4, CH	6.81, d (8.0)	3, 6, 8	125.7, CH	6.91, d (8.5)	6, 8	120.4, CH	6.79, d (8.5)	3, 6, 8
5	117.7, CH	6.71, d (8.0)	6, 7, 9	110.0, CH	6.48, d (8.0)	7, 9	117.7, CH	6.71, d (8.5)	6, 7, 9
6	146.3, C			153.3, C			146.3, C		
7	135.4, C			105.3, C			135.4, C		
8	132.2, C			137.0,C			132.3, C		
9	124.4, C			120.6, C			124.5, C		
10	37.0, CH_2	2.81, d (15.5)	2, 3, 11, 12, 21	37.2, CH_2	2.78, d (15.5)	2, 3, 11, 12, 21	39.6, CH_2	2.42, d (15.5)	2, 3, 11, 12, 21
		2.02, d (15.5)	2, 3, 9, 11, 12, 20		2.00, d (15.5)	2, 3, 9, 11, 12		2.13, d (15.5)	2, 3, 9, 11, 12, 20
11	64.7, C			64.6, C			61.4, C		
12	49.2, CH_2	3.82, d (12.0)		49.2, CH_2	3.81, d (12.0)		49.5,CH_2	3.83, d (11.5)	
		3.50, d (12.5)	11, 20		3.50, d (12.5)	11, 20		3.56, d (11.5)	11, 20
13	63.0, C			63.2, C			63.6, C		
14	31.4, CH_2	2.61, dd (13.5, 6.0)	13, 15, 16, 17, 18, 19	31.4, CH_2	2.61, dd (13.5, 5.5)	13, 15, 17, 18, 19	30.7, CH_2	2.55, dd (13.0, 6.0)	13, 15, 17, 18, 19
		2.08, dd (13.5, 10.0)	13, 15, 16, 17, 18, 19		2.08, dd (13.5, 9.5)			2.05, dd (12.5, 10.0)	13, 15, 17, 18, 19
15	37.2, C	2.73, m	14, 16, 17	37.0, C	2.73, m		37.4, C	2.71, m	16, 17
16	175.3, C			175.3, C			175.3, C		
17	17.1, CH_3	1.25, d (7.0)	14, 15, 16	17.1,CH_3	1.25, d (7.5)	14, 15, 16	17.2,CH_3	1.25, d (7.5)	14, 15, 16
18	171.9, C			172.0, C			174.0, C		
19	29.8, CH_2	1.94, dd (12.5, 11.0)	11, 20	30.1, CH_2	1.94, dd (12.5, 11.0)		29.7, CH_2	1.97, dd (12.0, 11.0)	11, 20
		1.79, dd (12.5, 10.5)	13, 18, 20, 21		1.79, dd (12.5, 10.5)			1.79, dd (12.5, 11.0)	13, 18, 20, 21
20	53.3, CH	3.33, t (10.5)	11, 12, 19, 21, 22, 23	53.5, CH	3.29, t (10.5)		54.6, CH	3.32, t (10.5)	11, 12, 19, 21, 22, 23
21	46.2, C			46.1, C			46.2, C		
22	20.7, CH_3	1.08, s	3, 20, 21, 23	20.6, CH_3	1.08, s	3, 20, 21, 23	20.7, CH_3	1.07, s	3, 20, 21, 23
23	23.9, CH_3	0.87, s	3, 20, 21, 22	23.8, CH_3	0.86, s	3, 20, 21, 22	24.0, CH_3	0.87, s	3, 20, 21, 22
24	138.9, CH	6.31, d (7.5)	7, 25, 26	115.8, CH	6.29, d (10.0)	26	138.9, CH	6.31, d (7.5)	7, 25, 26
25	115.3, CH	4.90, d (7.5)	24, 26, 27, 28	131.5, CH	5.72, d (10.0)	7, 26	115.3, CH	4.89, d (8.0)	24, 26, 27, 28
26	79.9, C			76.4, C			79.9, C		
27	30.0, CH_3	1.46, s	25, 26, 28	27.8,CH_3	1.47, s	25, 26, 28	30.1, CH_3	1.46, s	25, 26, 28
28	30.0, CH_3	1.44, s	25, 26, 27	28.0, CH_3	1.43, s	25, 26, 27	30.2, CH_3	1.43, s	25, 26, 27
29	27.3, CH_3	3.10, s	11, 18	27.2, CH_3	3.09, s	11, 18			
NH-1		7.81, s	3, 8, 9		8.43, s			7.83, s	3, 8, 9
NH-29								6.97, s	13

[a]$CDCl_3$. [b]HMBC correlations, optimized for 8 Hz.

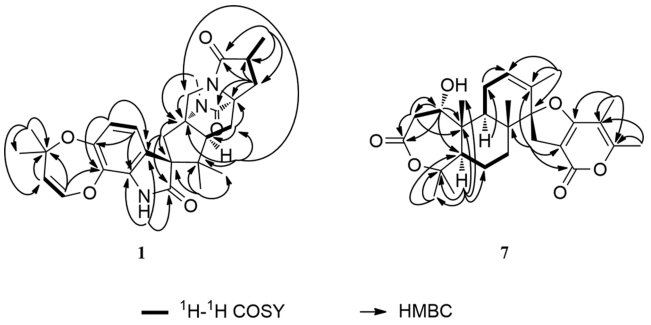

Figure 1. HMBC and COSY correlations of compounds 1 and 7.

1.50 (3H, s, Me-18), 1.48 (3H, s, Me-19), 1.14 (3H, s, Me-20), and 0.96 (3H, s, Me-17)], five methylene groups [δ_H 3.23 (1H, d, J = 15.5 Hz, H-2a), 3.03 (1H, d, J = 15.0 Hz, H-15a), 2.94 (1H, d, overlapped, H-2b), 2.92 (1H, d, J = 15.0 Hz, H-15b), 2.17 (1H, m, H-11a), 2.02 (1H, m, H-11b), 1.69 (1H, m, H-6a), 1.59 (1H, m, H-6b), 1.56 (1H, m, H-7a), and 1.43 (1H, m, H-7b)], and four methine groups, including one olefinic [δ_H 5.65 (1H, m, H-12), 3.83 (1H, d, J = 5.0 Hz, H-1), 2.61 (1H, dd, J = 11.0, 5.0 Hz, H-9), and 2.01 (1H, d, J = 11.0 Hz, H-5)]. The ^{13}C NMR spectroscopic data (Table 3) showed 27 carbon signals, including seven methyl, four methine, five methylene, two carbonyl, four oxygenated tertiary, and five quaternary carbons. These 1D NMR data of 7 were similar to those of brevione C,[19] which has a pentacyclic carbon framework consisting of a diterpenoid and a polyketide moiety, except for the replacement of a 3-methylcyclohept-2,6-dienone ring by a 4-hydroxy-7,7-dimethyloxepan-2-one ring in 7 [3.83 (1H, d, J = 5.0 Hz, H-1), 3.23 (1H, d, J = 15.5 Hz, H-2a), 2.94 (1H, d, overlapped, H-2b), 1.50 (3H, s, Me-18), and 1.48 (3H, s, Me-19)].[11] These data were confirmed by the HMBC correlations

DOI: 10.1021/acs.jnatprod.5b00508
J. Nat. Prod. XXXX, XXX, XXX−XXX

Table 2. NMR Spectroscopic Data of Compounds 4−6

	4[a]			5[b]			6[b]		
position	δ_C, type	δ_H, mult (J in Hz)	HMBC[c]	δ_C, type	δ_H, mult (J in Hz)	HMBC[c]	δ_C, type	δ_H, mult (J in Hz)	HMBC[c]
2	184.0, C			183.2, C			184.2, C		
3	62.6, C			63.5, C			62.7, C		
4	125.6, CH	6.89, d (8.0)	3, 6, 8	121.8, CH	7.05, d (8.5)	6, 8	126.9, CH	7.11, d (8.5)	6, 8
5	109.9, CH	6.48, d (8.0)	6, 7, 9	117.5, CH	6.67, d (8.0)	6, 7, 9	109.5, CH	6.39, d (8.5)	7, 9
6	153.3, C			147.2, C			153.8, C		
7	105.5, C			136.4, C			106.0, C		
8	137.1, C			134.4, C			139.4, C		
9	120.7, C			126.9,C			122.9, C		
10	39.5, CH_2	2.36, d (15.0)	2, 11	38.1, CH_2	2.69, d (15.5)	2, 3, 11, 12, 21	38.1, CH_2	2.66, d (15.5)	2, 3, 11, 12, 21
		2.11, d (15.5)	2, 9, 11, 12		1.96, d (15.0)	2, 3, 9, 11, 12, 20		1.91, d (15.5)	2, 9, 11, 12, 20
11	61.4, C			65.8, C			65.7, C		
12	49.4, CH_2	3.81, d (11.5)		59.8, CH_2	3.64, d (11.0)		59.9, CH_2	3.63, d (11.0)	
		3.56, d (12.0)	11, 20		2.62, d (11.5)			2.62, d (11.0)	
13	63.7, C			68.1, C			68.2, C		
14	30.7, CH_2	2.54, dd (13.5, 5.0)	13, 15, 17, 18, 19	36.8, CH_2	2.23, dd (12.5, 5.5)	18	36.8, CH_2	2.24, dd (12.5, 5.0)	13, 15, 17, 18
		2.05, dd (13.0, 10.0)	18, 19		1.57, dd (12.0, 10.5)			1.58, dd (12.0, 10.5)	
15	37.4, C	2.72, m		32.4, C	2.30, m		32.4, C	2.30, m	
16	175.2, C			62.6, CH_2	3.06, m	13, 14	62.7, CH_2	3.06, m	13, 14
					1.79, m			1.79, m	
17	17.2, CH_3	1.24, d (7.5)	14, 15, 16	19.5, CH_3	1.00, d (7.0)	14, 15, 16	19.5, CH_3	0.99, d (7.0)	14, 15, 16
18	174.3, C			174.1, C			174.0, C		
19	30.2, CH_2	1.96, dd (12.5, 11.0)		30.4, CH_2	1.73, dd (12.5, 11.0)	11	30.3, CH_2	1.72, dd (12.0, 11.0)	
		1.79, dd (12.0, 11.0)			1.71, dd (12.0, 11.0)	20		1.69, dd (12.0, 11.0)	
20	54.9, CH	3.32, t (10.5)		53.7, CH	3.04, t (10.5)		53.8, CH	3.04, t (10.5)	
21	46.1, C			46.5, C			46.4, C		
22	20.5, CH_3	1.06, s	3, 20, 21, 23	21.0, CH_3	1.12, s	3, 20, 21, 23	20.9, CH_3	1.11, s	3, 20, 21, 23
23	23.8, CH_3	0.84, s	3, 20, 21, 22	24.4, CH_3	0.81, s	3, 20, 21, 22	24.3, CH_3	0.80, s	3, 20, 21, 22
24	116.0, CH	6.35, d (10.5)	26	140.0, CH	6.37, d (7.5)	7, 25, 26	117.6, CH	6.67, d (10.0)	26
25	131.4, CH	5.73, d (10.0)	7, 26	116.0, CH	4.97, d (8.0)	24, 26	131.2, CH	5.76, d (9.5)	7, 26
26	76.4, C			80.3, C			76.6, C		
27	28.0, CH_3	1.47, s	25, 26, 28	29.9, CH_3	1.43, s	25, 26, 28	28.1, CH_3	1.42, s	25, 26, 28
28	27.8, CH_3	1.43, s	25, 26, 27	31.3, CH_3	1.41, s	25, 26, 27	28.0, CH_3	1.41, s	25, 26, 27
29				26.2, CH_3	3.03, s	11, 18	26.2, CH_3	3.02, s	11, 18
NH-1		8.47, s			9.43, s			9.53, s	
NH-29		6.95, s	13						

[a]$CDCl_3$. [b]Acetone-d_6. [c]HMBC correlations, optimized for 8 Hz.

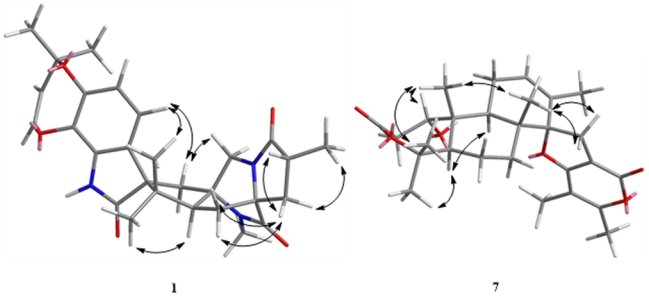

Figure 2. Key NOESY correlations of compounds **1** and **7**.

of Me-20/C-1, C-5, C-9, and C-10 and of Me-18, -19/C-4 and C-5 (Figure 1). The entire structure of the new compound **7** was established by additional 2D NMR studies and elucidated as brevione L.

Compound **8** (brevione M) showed a molecular ion peak at m/z 439.2485 $[M + H]^+$ in the HRESIMS, consistent with the molecular formula $C_{27}H_{34}O_5$. The ^1H and ^{13}C NMR data of **8** (Table 3) were similar to those of **7** and suggested that **8** was a dehydrated form of **7**, as indicated by the olefinic proton signals [δ_H 6.46 (1H, d, J = 12.5 Hz, H-1) and 5.89 (1H, d, J = 12.0 Hz, H-2)] and the HMBC cross-peaks of Me-20/C-1 and H-9/C-1.

The relative configurations of compounds **7** and **8** were the same as those of the previously reported spiroditerpenoids, as indicated by the close similarity of the ^1H and ^{13}C chemical shifts and NOESY data.[19,20] The NOESY correlations of H-5/H-9 and Me-19 suggested that these protons were on the same face of the ring system; those of Me-17/H-15 and Me-20 and of Me-18/Me-20 supported their positioning on the opposite face of the system (Figure 2). The absolute configurations of compounds **7** and **8** were established by comparing their

DOI: 10.1021/acs.jnatprod.5b00508
J. Nat. Prod. XXXX, XXX, XXX−XXX

Table 3. NMR Spectroscopic Data of Compounds 7 and 8

	7[a]			8[a]		
position	δ_C, type	δ_H, mult (J in Hz)	HMBC[b]	δ_C, type	δ_H, mult (J in Hz)	HMBC[b]
1	68.7, CH	3.83, d (5.0)	2, 3, 5, 10	156.1, CH	6.46, d (12.5)	5, 9
2	39.0, CH_2	3.23, d (15.5)	1, 3, 10	120.5, CH	5.89, d (12.0)	3, 10
		2.94, overlapped	1, 3, 10			
3	172.0, C			167.6, C		
4	86.0, C			85.3, C		
5	49.6, CH	2.01, d (11.0)	4, 6, 10, 18, 20	56.1, CH	1.98, m	4, 6, 10, 20
6	21.2, CH_2	1.69, m		22.2, CH_2	1.63, m	
		1.59, m	5			
7	31.7, CH_2	1.56, m	5, 6, 9	31.6, CH_2	1.56, m	
		1.43, m	6, 8, 14, 17		1.38, m	
8	40.7, C			41.1, C		
9	39.0, CH	2.61, dd (11.0, 5.0)	1, 8, 10, 11, 14, 20	45.1, CH	1.95, m	1, 8, 10, 11, 17, 20
10	44.8, C			43.5, C		
11	23.1, CH_2	2.17, m	8, 12, 13	24.2, CH_2	2.19, m	
		2.02, m				
12	127.6, CH	5.65, m	9, 11, 14, 16	127.3, CH	5.69, m	
13	131.7, C			132.1, C		
14	99.6, C			99.5, C		
15	28.8, CH_3	3.03, d (15.0)	8, 13, 1′, 2′	28.7, CH_3	3.03, d (16.0)	8, 13, 1′, 2′
		2.92, d (15.0)	8, 13, 1′, 2′		2.91, d (15.5)	8, 13, 1′, 2′
16	18.5, CH_3	1.66, s	12, 13, 14	18.2, CH_3	1.65, s	12, 13, 14
17	16.5, CH_3	0.96, s	7, 8, 9, 14	16.2, CH_3	1.00, s	7, 8, 9, 14
18	23.8, CH_3	1.50, s	4, 5, 19	26.4, CH_3	1.47, s	4, 5, 19
19	34.5, CH_3	1.48, s	4, 5, 18	32.2, CH_3	1.44, s	4, 5, 18
20	15.6, CH_3	1.14, s	1, 5, 9, 10	15.5, CH_3	1.32, s	1, 5, 9, 10
1′	171.2 C			171.0, C		
2′	99.3, C			99.2, C		
3′	162.0, C			161.9, C		
4′	103.0, C			102.9, C		
5′	160.5, C			160.6, C		
6′	9.7, CH_3	1.93, s	1′, 4′, 5′	9.8, CH_3	1.93, s	1′, 4′, 5′
7′	17.2, CH_3	2.22, s	4′, 5′	17.2, CH_3	2.22, s	4′, 5′

[a]$CDCl_3$. [b]HMBC correlations, optimized for 8 Hz.

experimental CD spectra with those calculated using the time-dependent density functional theory (TDDFT) method.[21] The optimized geometries were attained by a conformational search with the MMFF94 force field and optimized at the B3LYP/6-31+G(d) level by the Gaussian 09 software package.[22] After optimization, the theoretical ECD spectra were calculated at the CAM-B3LYP/SVP level with a CPCM solvent model in MeOH. The calculated ECD spectra of **7** and **8** showed a good fit with the respective experimental results (Figure 3), confirming the absolute configuration of compound **7** as 1*S*, 5*R*, 8*R*, 9*R*, 10*R*, and 14*S* and that of compound **8** as 5*R*, 8*R*, 9*R*, 10*R*, and 14*S*.

All isolated compounds were tested for their inhibition of Aβ aggregate-induced toxicity in PC12 cells and Aβ aggregation using an MTT assay[23] and a thioflavin T assay,[24] respectively. The EC_{50} and IC_{50} values of these compounds are presented in Table 4. Rosmarinic acid was used as a reference compound due to its potency on Aβ aggregation and Aβ-induced toxicity.[25] Only compounds **8**−**11** efficiently protected the cells from Aβ-induced toxicity. Among the active compounds, **8** exhibited the highest activity, with an EC_{50} value of 65.4 μM, which is comparable to rosmarinic acid.

On the other hand, compounds **4**−**6** and **9** exhibited moderate inhibitory effects on Aβ aggregation (Table 4). These compounds inhibited Aβ aggregation by 30% at 100 μM. Among the active compounds, **4** and **5** did not protect the cells against Aβ-induced toxicity, and **9** was the only one having inhibitory activities of both Aβ-induced toxicity and Aβ aggregation, whereas **6** was cytotoxic to PC12 cells.

Three compounds (**4**, **5**, and **9**) were selected to evaluate whether their observed inhibition of Aβ aggregation could rescue the cells from Aβ aggregate-induced toxicity (Table 5). Particularly, incubating Aβ monomers with **4** and **5** protected the cells from Aβ aggregate-induced toxicity, even though these compounds did not exhibit any protective effects against Aβ aggregate-induced toxicity. These results indicated that incubation of Aβ monomers with **4** and **5** reduces their aggregation and parts of Aβ exist as monomers, and this process rescues the cells from neurotoxic Aβ aggregates. Therefore, **4** and **5** exerted their effects by inhibiting the formation of neurotoxic aggregates from Aβ monomers, but not by inhibiting Aβ aggregate-induced neurotoxicity. On the other hand, incubating Aβ monomers with **9** protected the cells from Aβ aggregate-induced toxicity, with the lowest EC_{50} value of 89.9 μM, indicating that the effects of **9** on both inhibition of Aβ aggregation and Aβ aggregate-induced toxicity work synergistically to protect cells from neurotoxic Aβ.

Aβ is produced by the sequential proteolysis of amyloid precursor proteins by β- and γ-secretases.[2] This process secretes Aβ monomers out of the neurons, and the self-aggregation of

DOI: 10.1021/acs.jnatprod.5b00508
J. Nat. Prod. XXXX, XXX, XXX−XXX

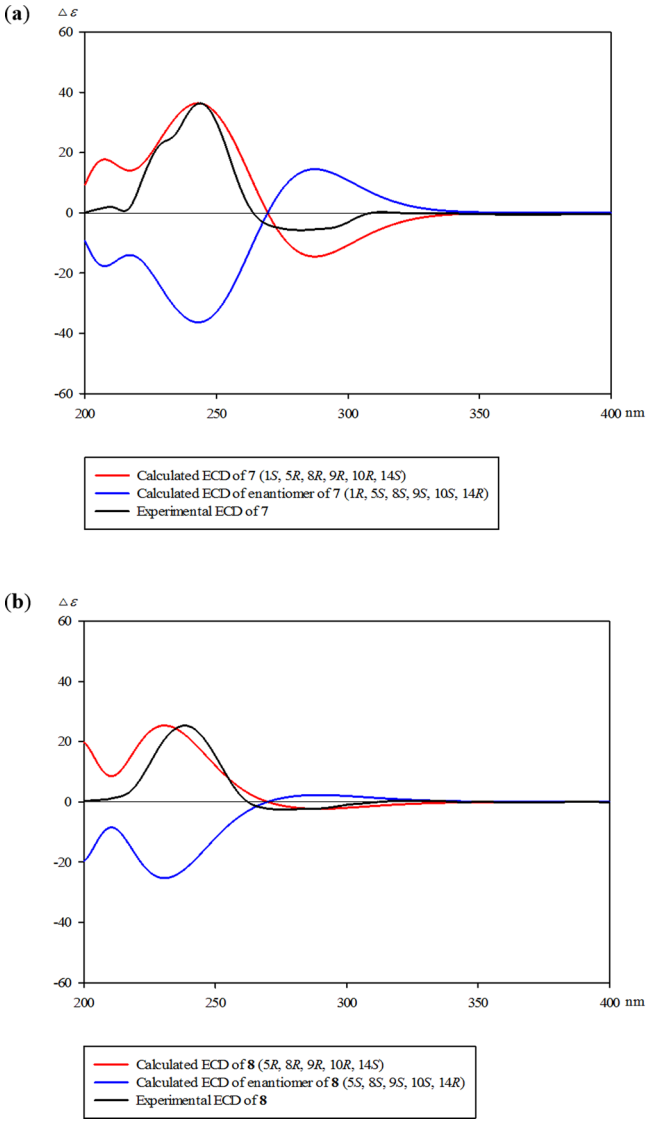

Figure 3. Calculated and experimental ECD spectra of compounds **7** (a) and **8** (b).

Table 4. Inhibition of Aβ Aggregate-Induced Toxicity and Aβ Aggregation by Compounds 1−11

compound	Aβ aggregate-induced neurotoxicity in PC12 cells[a]	Aβ aggregation[b]
1	>300.0	>300.0
2	>300.0	>300.0
3	>300.0	>300.0
4	>300.0	244.3
5	>300.0	269.5
6	>300.0	203.7
7	>300.0	>300.0
8	65.4	>300.0
9	149.6	186.6
10	112.6	>300.0
11	251.5	>300.0
rosmarinic acid[c]	68.1	71.9

[a]EC_{50} is expressed in μM as means of triplicate experiments. [b]IC_{50} is expressed in μM as means of triplicate experiments. [c]Positive control.

Table 5. Inhibition of Aβ Aggregation by the Selected Compounds Protecting Cells from Aβ Aggregate-Induced Toxicity

compound	cell viability[a]
4	97.9
5	105.2
9	89.9
rosmarinic acid[b]	57.2

[a]EC_{50} is expressed in μM as means of triplicate experiments. [b]Positive control.

Aβ monomers generates Aβ oligomers, which are the neurotoxic form of Aβ found in AD.[3] The cognitive decline in AD patients is related to the levels of Aβ aggregates in cerebrospinal fluid.[26] For example, α-tocopherol quinine improved the spatial memory of AD transgenic mice by reducing Aβ aggregation.[27] Tramiprosate, which is a small glycosaminoglycan minetic inhibiting Aβ fibril formation, was applied to the phase III trial. Even though the results did not demonstrate statistical significance between mild-to-moderate AD and control groups, post hoc adjusted analyses showed the positive effects on the reduction of hypocampal volume and cognitive decline.[28] The increasing evidence supports that inhibitors of Aβ aggregation are beneficial for AD treatment.[29] In this study, compounds **8** and **11** protected the cells from Aβ aggregate-induced toxicity, but did not inhibit the aggregation of Aβ. Compounds **4** and **5** did not block Aβ aggregate-induced toxicity, but reduced the formation of Aβ aggregates and increased Aβ monomers. Compound **9** exhibited both activities, resulting in the best protective effect on PC12 cells. These results suggest that these compounds have a potential to be developed as antiamyloidogenic agents. Particularly, compound **9**, which has inhibitory activities against both Aβ aggregation and Aβ-induced toxicity, may deserve further research as a potential therapeutic or preventative agent in AD.

EXPERIMENTAL SECTION

General Experimental Procedures. Optical rotations were measured on a Jasco P-2000 with a 10 mm cell. The UV spectra were obtained using a Mecasys Optizen pop spectrometer, and IR spectra were carried out on a Varian 640 FT-IR spectrometer. NMR spectroscopic data were recorded at room temperature on a Varian 500 MHz NMR spectrometer with tetramethylsilane as an internal standard. ESI-Tof-MS data were obtained with a Waters Q-TOF micromass spectrometer. CD spectra were obtained using a Jasco J-810 spectropolarimeter. High-speed countercurrent chromatography (HSCCC) was conducted on TBE-20A and TBE-1000A systems with a Shimadzu UV detector. HPLC was performed using a Waters system comprising a 515 pump and a 2996 PDA detector with a YMC Pack ODS-A column (5 μm, 250 × 20 mm i.d).

Fungus Cultivation. *A. duricaulis* KACC 41137 (Raper & Fennell) was obtained from the Korean Agricultural and Culture Collection (http://www.genebank.go.kr), Wanju, Korea, and cultivated in Petri dishes (150 mm × 2 cm × 150 plates) on potato dextrose agar media at 25 °C for 21 days.

Extraction and Isolation. The fermented materials were extracted with MeOH (3 × 2 L) at room temperature, and the crude extracts were evaporated *in vacuo* at 35 °C. The residue was suspended in H_2O (2 L) and then partitioned with EtOAc (4 × 2 L) to give EtOAc-soluble extract (650.0 mg). Accordingly, the EtOAc extract was fractionated by preparative HSCCC (*n*-hexane−EtOAc−MeOH−H_2O, 3:7:5:5, flow rate 10.0 mL/min, rotation speed 500 rpm) to yield 10 fractions (Fr 1 to Fr 10). Fr 2 (20.8 mg) was purified by preparative HPLC (MeCN−H_2O, 7:13 to 1:1, flow rate 8.0 mL/min) to yield 29-*N*-demethylparaherquamide J (**3**, 5.5 mg), 29-*N*-

DOI: 10.1021/acs.jnatprod.5b00508
J. Nat. Prod. XXXX, XXX, XXX−XXX

demethylparaherquamide K (**4**, 1.7 mg), brevione L (**7**, 2.1 mg), and 16-oxo-paraherquamide B (**9**, 2.1 mg). Fr 3 (60.8 mg) was separated by preparative HPLC (MeCN−H_2O, 7:13 to 1:1, flow rate 8.0 mL/min) to give paraherquamide J (**1**, 39.6 mg), paraherquamide K (**2**, 6.4 mg), and setosusin (**10**, 1.0 mg). Fr 5 (23.0 mg) was purified by preparative HPLC (MeCN−H_2O, 1:4 to 7:3, flow rate 8.0 mL/min) to afford 16-deoxo-paraherquamide J (**5**, 6.4 mg). Fr 6 (18.3 mg) was separated by preparative HPLC (MeCN−H_2O, 1:4 to 7:3, flow rate 8.0 mL/min) to yield 16-deoxo-paraherquamide K (**6**, 2.5 mg) and brevione M (**8**, 2.2 mg). Fr 7 (9.8 mg) was purified by preparative HPLC (MeCN−H_2O, 7:13 to 1:1, flow rate 8.0 mL/min) to give 4-hydroxy-3-prenylbenzoic acid (1.7 mg). Fr 8 (18.6 mg) was separated by preparative HPLC (MeCN−H_2O, 1:4 to 7:3, flow rate 8.0 mL/min) to afford deacetyl-dehydrated setosusin (7.9 mg) and 2,2-dimethyl-2*H*-1-chromene-6-carboxylate (**11**, 1.5 mg).

*Paraherquamide J (**1**):* colorless, amorphous powder; $[\alpha]^{23}_D$ −50.1 (*c* 0.04, MeOH); UV (MeOH) λ_{max} (log ε) 225 (4.4) nm; IR ν_{max} (ATR) 2973, 1671, 1462, 1385, 1197, 1048 cm^{-1}; CD (c 0.3 mM, MeOH) $\Delta\varepsilon$ +64.1 (244), −70.6 (262), −15.2 (292); ^{13}C and ^1H NMR (500 and 125 MHz, $CDCl_3$), see Table 1; NOESY correlations H-4/H-10b, Me-22; H-5/Me-27, Me-28; H-10a/H-10b, Me-29; H-10b/H-4, H-10a, H-12a, H-12b, Me-22; H-12a/H-10b, H-12b, Me-22; H-14a/H-14b, Me-17; H-14b/H-14a, H-15, H-19a, H-19b; H-15/H-14b, Me-17; Me-17/H-14a, H-15; H-19a/H-19b, H-20; H-19b/H-19a, Me-22; H-20/H-19a, Me-23; Me-22/H-4, H-10b, H-12a, H-19b, Me-23; Me-23/H-20, Me-22; H-24/H-25; H-25/H-24, Me-27, Me-28; Me-27/H-5, H-25; Me-28/H-5, H-25; Me-29/H-10a; ESIMS (negative) *m*/*z* 490 $[M - H]^-$; ESIMS (positive) *m*/*z* 492 $[M + H]^+$; HRESIMS *m*/*z* 492.2478 $[M + H]^+$ (calcd for $C_{28}H_{34}N_3O_5$, 492.2498).

*Paraherquamide K (**2**):* colorless, amorphous powder; $[\alpha]^{23}_D$ −43.7 (*c* 0.04, MeOH); UV (MeOH) λ_{max} (log ε) 245 (3.8) nm; IR ν_{max} (ATR) 2924, 1685, 1457, 1382, 1207, 1057 cm^{-1}; CD (c 0.3 mM, MeOH) $\Delta\varepsilon$ −65.7 (225), −28.8 (272); ^{13}C and ^1H NMR (500 and 125 MHz, $CDCl_3$), see Table 1; NOESY correlations H-4/H-5, H-10b, Me-22; H-5/H-4, Me-27, Me-28; H-10a/H-10b, Me-29; H-10b/H-4, H-10a, H-12a, H-12b, Me-22; H-12a/H-10b, H-12b, Me-22; H-14a/H-14b, Me-17; H-14b/H-14a, H-15, H-19a, H-19b; H-15/H-14b, Me-17; Me-17/H-14a, H-15; H-19a/H-19b, H-20; H-19b/H-19a, Me-22; H-20/H-19a, Me-23; Me-22/H-4, H-12a, H-19b, Me-23; Me-23/H-20, Me-22; H-24/H-25; H-25/H-24, Me-27, Me-28; Me-27/H-25; Me-28/H-25; Me-29/H-10a; ESIMS (negative) *m*/*z* 474 $[M - H]^-$; ESIMS (positive) *m*/*z* 476 $[M + H]^+$; HRESIMS *m*/*z* 476.2535 $[M + H]^+$ (calcd for $C_{28}H_{34}N_3O_4$, 476.2549).

*29-N-Demethylparaherquamide J (**3**):* colorless, amorphous powder; $[\alpha]^{23}_D$ −56.3 (*c* 0.05, MeOH); UV (MeOH) λ_{max} (log ε) 225 (4.4) nm; IR ν_{max} (ATR) 2938, 1673, 1462, 1332, 1199, 1048 cm^{-1}; CD (*c* 0.2 mM, MeOH) $\Delta\varepsilon$ +47.2 (243), −52.8 (262), −12.3 (288); ^{13}C and ^1H NMR (500 and 125 MHz, $CDCl_3$), see Table 1; NOESY correlations H-4/H-10b, Me-22; H-5/Me-27, Me-28; H-10a/H-10b, Me-29; H-10b/H-4, H-10a, H-12a, H-12b, Me-22; H-12a/H-10b, H-12b, Me-22; H-14a/H-14b, Me-17; H-14b/H-14a, H-15, H-19a, H-19b; H-15/H-14b, Me-17; Me-17/H-14a, H-15; H-19a/H-19b, H-20; H-19b/H-19a, Me-22; H-20/H-19a, Me-23; Me-22/H-4, H-10b, H-12a, H-19b; Me-23/H-20, Me-22; H-24/H-25; H-25/H-24, Me-27, Me-28; Me-27/H-25; Me-28/H-25; H-29/H-10a, H-20; ESIMS (negative) *m*/*z* 476 $[M - H]^-$; ESIMS (positive) *m*/*z* 478 $[M + H]^+$; HRESIMS *m*/*z* 478.2322 $[M + H]^+$ (calcd for $C_{27}H_{32}N_3O_5$, 478.2342).

*29-N-Demethylparaherquamide K (**4**):* colorless, amorphous powder; $[\alpha]^{23}_D$ −37.5 (*c* 0.04, MeOH); UV (MeOH) λ_{max} (log ε) 245 (4.1) nm; IR ν_{max} (ATR) 2921, 1684, 1457, 1364, 1205, 1058 cm^{-1}; CD (c 0.2 mM, MeOH) $\Delta\varepsilon$ −67.5 (227), −24.4 (275); ^{13}C and ^1H NMR (500 and 125 MHz, $CDCl_3$), see Table 2; NOESY correlations H-4/H-10b, Me-22; H-5/Me-27, Me-28; H-10a/H-10b; H-10b/H-4, H-10a, H-12a, H-12b, Me-22; H-12a/H-10b, H-12b, Me-22; H-14a/H-14b, Me-17; H-14b/H-14a, H-15; H-15/H-14b, Me-17; Me-17/H-14a, H-15; H-19a/H-19b; H-19b/H-19a, Me-22; H-20/H-19a, Me-23; Me-22/H-4, H-12a, H-19b, Me-23; Me-23/H-20; H-24/H-25; H-25/H-24, Me-27, Me-28; Me-27/H-25; Me-28/H-25; ESIMS (negative) *m*/*z* 460 $[M - H]^-$; ESIMS (positive) *m*/*z* 462 $[M + H]^+$; HRESIMS *m*/*z* 462.2409 $[M + H]^+$ (calcd for $C_{27}H_{32}N_3O_4$, 462.2393).

*16-Deoxo-paraherquamide J (**5**):* colorless, amorphous powder; $[\alpha]^{23}_D$ −70.3 (*c* 0.05, MeOH); UV (MeOH) λ_{max} (log ε) 225 (4.4) nm; IR ν_{max} (ATR) 2927, 1670, 1491, 1327, 1199, 1048 cm^{-1}; CD (*c* 0.2 mM, MeOH) $\Delta\varepsilon$ +51.9 (239), −38.2 (264), −6.4 (293); ^{13}C and ^1H NMR (500 and 125 MHz, acetone-d_6), see Table 2; NOESY correlations H-4/H-5, H-10b, Me-22; H-5/H-4, Me-27, Me-28; H-10a/H-10b, Me-29; H-10b/H-4, H-10a, H-12a, H-12b, Me-22; H-12a/H-10b, H-12b, Me-22; H-14a/H-14b, Me-17; H-14b/H-14a, H-15, H-19b; H-15/H-14b, Me-17; H-16a/H-16b; H-16b/H-12b, H-16a, Me-17; Me-17/H-14a, H-15; H-19a/H-19b, H-20; H-19b/H-19a, Me-22; H-20/H-19a, Me-23; Me-22/H-4, H-10b, H-12a, H-19b, Me-23; Me-23/H-20, Me-22; H-24/H-25; H-25/H-24, Me-27, Me-28; Me-27/H-25; Me-28/H-25; Me-29/H-10a; ESIMS (negative) *m*/*z* 476 $[M - H]^-$; ESIMS (positive) *m*/*z* 478 $[M + H]^+$; HRESIMS *m*/*z* 478.2688 $[M + H]^+$ (calcd for $C_{28}H_{36}N_3O_4$, 478.2706).

*16-Deoxo-paraherquamide K (**6**):* colorless, amorphous powder; $[\alpha]^{23}_D$ −16.7 (*c* 0.02, MeOH); UV (MeOH) λ_{max} (log ε) 245 (3.8) nm; IR ν_{max} (ATR) 2922, 1677, 1454, 1204, 1138, 1058 cm^{-1}; CD (*c* 0.1 mM, MeOH) $\Delta\varepsilon$ −20.5 (228), −15.3 (275); ^{13}C and ^1H NMR (500 and 125 MHz, acetone-d_6), see Table 2; NOESY correlations H-4/H-5, H-10b, Me-22; H-5/H-4; H-10a/H-10b, Me-29; H-10b/H-10a, H-12a, H-12b; H-12a/H-10b, H-12b, Me-22; H-14a/H-14b, Me-17; H-14b/H-14a, H-15; H-16a/H-16b; H-16b/H-12b, H-16a, Me-17; Me-17/H-14a, H-15; H-19a/H-14b, H-19b, H-20; H-19b/Me-22; H-20/H-19a, Me-23; Me-22/H-4, H-12a, H-19b, Me-23; Me-23/H-20, Me-22; H-24/H-25; H-25/H-24, Me-27, Me-28; Me-29/H-10a; ESIMS (negative) *m*/*z* 460 $[M - H]^-$; ESIMS (positive) *m*/*z* 462 $[M + H]^+$; HRESIMS *m*/*z* 462.2774 $[M + H]^+$ (calcd for $C_{28}H_{36}N_3O_3$, 462.2757).

*Brevione L (**7**):* yellowish, amorphous powder; $[\alpha]^{23}_D$ +13.2 (*c* 0.02, MeOH); UV (MeOH) λ_{max} (log ε) 215 (4.2), 244 (3.5), 296 (3.6) nm; IR ν_{max} (ATR) 2934, 1693, 1573, 1443, 1217, 1126 cm^{-1}; CD (c 0.3 mM, MeOH) $\Delta\varepsilon$ +36.4 (244), −5.7 (280); ^{13}C and ^1H NMR (500 and 125 MHz, $CDCl_3$), see Table 3; NOESY correlations H-1/H-2a, H-2b, H-11a, Me-20; H-2a/H-1, H-2b, Me-18, Me-20; H-5/H-6a, H-7b, H-9, Me-19; H-6a/H-5, H-7a, H-7b; H-7a/H-6a, H-7b, H-15a, H-15b, Me-17; H-7b/H-5, H-6a; H-9/H-5, H-7b, H-11a; H-11a/H-1, H-12; H-11b/Me-17, Me-20; H-12/H-11a, H-11b, Me-16; H-15a/H-7a, Me-17; H-15b/Me-16, Me-17; Me-16/H-12, H-15b; Me-17/H-6b, H-11b, H-15a, Me-20; Me-18/H-2a, Me-20; Me-19/H-5, H-6a; Me-20/H-1, H-2a, H-6b, H-11b, Me-17, Me-18; Me-6′/Me-7′; Me-7′/Me-6′; ESIMS (negative) *m*/*z* 455 $[M - H]^-$; ESIMS (positive) *m*/*z* 457 $[M + H]^+$; HRESIMS *m*/*z* 457.2576 $[M + H]^+$ (calcd for $C_{27}H_{36}O_6$, 457.2590).

*Brevione M (**8**):* yellowish, amorphous solid; $[\alpha]^{23}_D$ +39.1 (*c* 0.02, MeOH); UV (MeOH) λ_{max} (log ε) 215 (4.1), 295 (3.3) nm; IR ν_{max} (ATR) 2925, 1689, 1574, 1443, 1200, 1132 cm^{-1}; CD (*c* 0.2 mM, MeOH) $\Delta\varepsilon$ +25.3 (238), −2.6 (276); ^{13}C and ^1H NMR (500 and 125 MHz, $CDCl_3$), see Table 3; NOESY correlations H-1/H-2, H-11, Me-20; H-2/H-1; H-5/H-6, H-7b, Me-19; H-6/H-5, H-7a, H-7b, Me-17, Me-20; H-7a/H-6, H-7b, H-15a, Me-17; H-7b/H-5, H-6; H-9/H-7b, H-11; H-11/H-1, H-12, Me-17, Me-20; H-12/H-11, Me-16; H-15a/H-7a, Me-17; H-15b/Me-16, Me-17; Me-16/H-12, H-15b; Me-17/H-6, H-11, H-15a, Me-20; Me-18/Me-20; Me-19/H-5, H-6; Me-20/H-1, H-6, H-11, Me-17, Me-18; Me-6′/Me-7′; Me-7′/Me-6′; ESIMS (negative) *m*/*z* 437 $[M - H]^-$; ESIMS (positive) *m*/*z* 439 $[M + H]^+$; HRESIMS *m*/*z* 439.2485 $[M + H]^+$ (calcd for $C_{27}H_{34}O_5$, 439.2484).

Computational Methods. Starting from the conformation of every compound deduced from NOESY spectra and Chem3D modelings, the conformational search with the MMFF94 force field was performed first using MOE software,[30] and the conformers were selected for geometry optimizations. Geometry optimizations and reoptimizations on the B3LYP/6-31+G(d) level were finished by the Gaussian 09 package.[22] TDDFT CD calculations for the optimized conformers were performed at the CAM-B3LYP/SVP level with a CPCM solvent model in methanol, and the calculated CD spectra of

DOI: 10.1021/acs.jnatprod.5b00508
J. Nat. Prod. XXXX, XXX, XXX−XXX

different conformers were simulated with a half bandwidth of ~0.4 eV. The CD curves were extracted by SpecDis 1.62 software.[31] The overall CD curves of all the compounds were weighted by Boltzmann distribution after UV correction.

Inhibition of Aβ Aggregate-Induced Toxicity. To test the protection of isolated compounds against Aβ-induced toxicity, PC12 cells (rat pheochromocytoma cells) were employed because PC12 cells are a commonly used cellular model to study neurodegenerative diseases.[32] PC12 cells obtained from Korea Cell Line Bank (Seoul, Korea) were cultured in RPMI 1640 medium (Welgene, Daegu, Korea) supplemented with 5% heat-inactivated fetal bovine serum (Equitech-BIO, Kerrville, TX, USA) and 15% heat-inactivated horse serum (Gibco BRL, Carlsbad, CA, USA) at 37 °C. PC12 cells were plated in 96-well plates with approximately 9×10^4 cells per well and incubated with various concentrations of all isolated compounds. After 1 h, 10 μM of aggregated $A\beta_{25-35}$ (Bachem AG, Bubendorf, Switzerland) was added into each well. Then the cells were incubated for an additional 24 h at 37 °C. Cell viability was determined using an MTT toxicity assay (Sigma-Aldrich, St. Louis, MO, USA).[23]

Inhibition of Aβ Aggregation. To quantify the aggregate formation of Aβ, the thioflavin T assay was performed.[24] The $A\beta_{1-42}$ (GL Biochem, Shanghai, China) was dissolved in DMSO at 1 mg/mL concentration. To monitor the effects of all isolated compounds on the aggregate formation of Aβ, 20 μM $A\beta_{1-42}$ was incubated with various concentrations of samples at 37 °C for 24 h. Then, 3 μM thioflavin T was added and fluorescence was measured after 30 min using an Emax precision microplate reader (Molecular Devices, CA, USA) with excitation at 442 nm and emission at 485 nm. The Aβ was used as a control, and each assay was performed in triplicate.

Protection of Cells by Inhibition of Aβ Aggregation. To monitor the effects of compounds inhibiting Aβ aggregation, three compounds (**4**, **5**, and **9**) were diluted with DMSO (4, 20, and 100 μg/mL) and incubated with 10 μM $A\beta_{1-42}$ at 37 °C. After 24 h, a mixture of compounds and Aβ was added to the PC12 cells. The cells were then incubated for an additional 24 h at 37 °C. Then the cell viability was determined using an MTT assay by adding 10 μL of 5 mg/mL MTT to the cells.[23] After 3 h of incubation, the medium was removed, and DMSO was added to the cells to dissolve the crystals. The absorbance was measured at 570 nm using an Emax precision microplate reader. The cell viability was calculated by dividing the absorbance with test compounds (corrected for background) by the absorbance with medium alone (corrected for background).

■ ASSOCIATED CONTENT

Supporting Information

The Supporting Information is available free of charge on the ACS Publications website at DOI: 10.1021/acs.jnatprod.5b00508.

^{1}H and ^{13}C NMR, MS, and CD spectra of new compounds and ^{1}H NMR data of known compounds (PDF)

■ AUTHOR INFORMATION

Corresponding Authors

*Tel: +82-41-550-1434. Fax: +82-41-559-7899. E-mail: soypark23@dankook.ac.kr (S.-Y. Park).

*Tel: +82-2-3290-3017. Fax: +82-2-953-0737. E-mail: dongholee@korea.ac.kr (D. Lee).

Notes

The authors declare no competing financial interest.

■ ACKNOWLEDGMENTS

This research was supported by a grant from the Korea Polar Research Institute (PM15050).

■ REFERENCES

(1) Huang, Y.; Mucke, L. *Cell* **2012**, *148*, 1204−1222.
(2) Park, S.-Y.; Kim, H.-S.; Hong, S. S.; Sul, D.; Hwang, K. W.; Lee, D. *Pharm. Biol.* **2009**, *47*, 976−981.
(3) Parihar, M. S.; Hemnani, T. *J. Clin. Neurosci.* **2004**, *11*, 456−467.
(4) Park, S.-Y. *Arch. Pharmacal Res.* **2010**, *33*, 1589−1609.
(5) Wimo, A.; Winblad, B.; Aguero-Torres, H.; von Strauss, E. *Alzheimer Dis. Assoc. Disord.* **2003**, *17*, 63−67.
(6) Finefield, J. M.; Frisvad, J. C.; Sherman, D. H.; Williams, R. M. *J. Nat. Prod.* **2012**, *75*, 812−833.
(7) Park, S.-Y.; Lim, J.-Y.; Jeong, W.; Hong, S. S.; Yang, Y. T.; Hwang, B. Y.; Lee, D. *Planta Med.* **2010**, *76*, 863−868.
(8) Lee, H. J.; Lyu, D. H.; Koo, U.; Lee, S.-J.; Hong, S. S.; Kim, K.; Kim, K. H.; Lee, D.; Mar, W. *Arch. Pharmacal Res.* **2011**, *34*, 1373−1380.
(9) Kwon, J.; Hiep, N. T.; Kim, D.-W.; Hwang, B. Y.; Lee, H. J.; Mar, W.; Lee, D. *J. Nat. Prod.* **2014**, *77*, 1893−1901.
(10) Lee, B. H.; Clothier, M. F. *J. Org. Chem.* **1997**, *62*, 1795−1798.
(11) Fujimoto, H.; Negishi, E.; Yamaguchi, K.; Nishi, N.; Yamazaki, M. *Chem. Pharm. Bull.* **1996**, *44*, 1843−1848.
(12) Baldoqui, D. C.; Kato, M. J.; Cavalheiro, A. J.; Bolzani, V. d. S.; Young, M. C. M.; Furlan, M. *Phytochemistry* **1999**, *51*, 899−902.
(13) Hayashi, K.; Komura, S.; Isaji, N.; Ohishi, N.; Yagi, K. *Chem. Pharm. Bull.* **1999**, *47*, 1521−1524.
(14) López-Gresa, M. P.; González, M. C.; Ciavatta, L.; Ayala, I.; Moya, P.; Primo, J. *J. Agric. Food Chem.* **2006**, *54*, 2921−2925.
(15) Blanchflower, S. E.; Banks, R. M.; Everett, J. R.; Manger, B. R.; Reading, C. *J. Antibiot.* **1991**, *44*, 492−497.
(16) Blanchflower, S. E.; Banks, R. M.; Everett, J. R.; Reading, C. *J. Antibiot.* **1993**, *46*, 1355−1363.
(17) Takayama, H.; Shimizu, T.; Sada, H.; Harada, Y.; Kitajima, M.; Aimi, N. *Tetrahedron* **1999**, *55*, 6841−6846.
(18) Greshock, T. J.; Grubbs, A. W.; Jiao, P.; Wicklow, D. T.; Gloer, J. B.; Williams, R. M. *Angew. Chem., Int. Ed.* **2008**, *47*, 3573−3577.
(19) Macías, F. A.; Varela, R. M.; Simonet, A. M.; Cutler, H. G.; Cutler, S. J.; Dugan, F. M.; Hill, R. A. *J. Org. Chem.* **2000**, *65*, 9039−9046.
(20) Li, Y.; Ye, D.; Shao, Z.; Cui, C.; Che, Y. *Mar. Drugs* **2012**, *10*, 497−508.
(21) Autschbach, J.; Nitsch-Velasquez, L.; Rudolph, M. *Top. Curr. Chem.* **2010**, *298*, 1−98.
(22) *Gaussian 09*, Revision B, 01; Gaussian, Inc.: Wallingford, CT, 2010.
(23) Kim, H.-Y.; Hwang, K. W.; Park, S.-Y. *Nutr. Res. (N. Y., NY, U. S.)* **2014**, *34*, 1008−1016.
(24) Wang, S.-w.; Wang, Y.-J.; Su, Y.-j.; Zhou, W.-w.; Yang, S.-g.; Zhang, R.; Zhao, M.; Li, Y.-n.; Zhang, Z.-p.; Zhan, D.-w.; Liu, R.-t. *NeuroToxicology* **2012**, *33*, 482−490.
(25) Ono, K.; Hasegawa, K.; Naiki, H.; Yamada, M. *J. Neurosci. Res.* **2004**, *75*, 742−750.
(26) Jongbloed, W.; Bruggink, K. A.; Kester, M. I.; Visser, P.-J.; Scheltens, P.; Blankenstein, M. A.; Verbeek, M. M.; Teunissen, C. E.; Veerhuis, R. *J. Alzheimers Dis.* **2014**, *45*, 35−43.
(27) Wang, S.-w.; Yang, S.-g.; Liu, W.; Zhang, Y.-x.; Xu, P.-x.; Wang, T.; Ling, T.-j.; Liu, R.-t. *Behav. Brain Res.* **2016**, *296*, 109−117.
(28) Aisen, P. S.; Gauthier, S.; Ferris, S. H.; Saumier, D.; Haine, D.; Garceau, D.; Duong, A.; Suhy, J.; Oh, J.; Lau, W. C. *Arch. Med. Sci.* **2011**, *7*, 102−111.
(29) Hefti, F.; Goure, W. F.; Jerecic, J.; Iverson, K. S.; Walicke, P. A.; Krafft, G. A. *Trends Pharmacol. Sci.* **2013**, *34*, 261−266.
(30) *MOE 2013.08*; Chemical Computing Group Inc., www.chemcomp.com.
(31) Bruhn, T.; Schaumlöffel, A.; Hemberger, Y.; Bringmann, G. *SpecDis* version 1.62; University of Wuerzburg: Germany, 2014.
(32) Vaudry, D.; Stork, P.; Lazarovici, P.; Eiden, L. *Science* **2002**, *296*, 1648−1649.

DOI: 10.1021/acs.jnatprod.5b00508
J. Nat. Prod. XXXX, XXX, XXX−XXX